

Shadow wave solutions for a scalar two-flux conservation law with Rankine-Hugoniot deficit

Tanja Krunić, Marko Nedeljkov

Abstract

The paper deals with scalar conservation laws having a flux discontinuity at $x = 0$ without a weak solution that satisfies the classical Rankine-Hugoniot jump condition at $x = 0$. We are using unbounded solutions in the form of shadow waves supported by the origin for solving that problem. The shadow waves are nets of piecewise constant functions approximating a shock wave with added a delta function and sometimes another unbounded part.

AMS Mathematics Subject Classification. 35L65, 35L67. *keywords:* conservation laws with discontinuous flux functions, shadow waves; delta shock waves, singular shock waves

1 Introduction

Suppose that a following scalar conservation law

$$\partial_t u + \partial_x f(x, u) = 0, \quad (1)$$

with a discontinuous flux function (“two flux functions”)

$$f(x, u) := H(x)f_r(u) + (1 - H(x))f_l(u) \quad (2)$$

is given. Here, $u = u(x, t) \in \Omega \subset \mathbb{R}$, $(x, t) \in \mathbb{R} \times \mathbb{R}_+$, $f_l, f_r \in C^1(\Omega)$ and $H(x)$ is the Heaviside step function. The functions f_l and f_r represent the left and right-hand sides of the flux jump. They are called “left” and “right flux” for short. The aim of this paper is to solve the cases when there is no a weak solution consisting of classical waves (shock or rarefaction waves) to the Riemann problem (2) with the initial data

$$u(x, 0) = \begin{cases} u_0, & x < 0 \\ u_1, & x > 0 \end{cases} . \quad (3)$$

For example, such a situation occurs when either f_l or f_r is of convex type, and the other of concave type and the graph of one of the parts of the flux jump lies below the other part (i.e. $f_l(u) >$ or $(<) f_r(u)$) on the entire domain Ω , see Fig. 1. Convex (concave) type function present a generalization of a convex

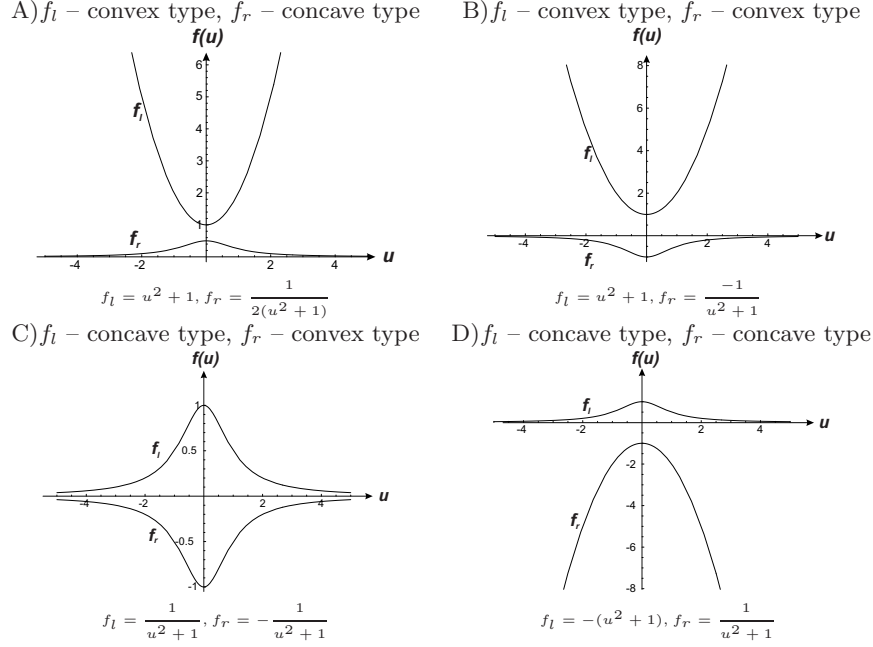


Figure 1: Examples of flux geometries with no classical solutions

(concave) function, the precise definition is given in Section 1.1. The reason why there is no solution is that the Rankine-Huginiot jump condition between two sides of the flux

$$f_l(u^-) = f_r(u^+), \quad (4)$$

with

$$u^- = \lim_{x \rightarrow 0^-} u(x, t) \quad \text{and} \quad u^+ = \lim_{x \rightarrow 0^+} u(x, t), \quad (5)$$

cannot be satisfied.

Our construction is based on solving the so-called overcompressive case first, i.e. the case when

$$f'_l(u_0) \geq 0 \geq f'_r(u_1). \quad (6)$$

Classical solutions of conservation laws with discontinuous flux functions have been widely investigated in the recent years. Equations of the form (1) are considered by many authors under the assumption that both fluxes f_l , f_r are of convex (concave) type. In these cases, equation (1) has weak solutions consisting of a left-going (backward) and a right-going (forward) shock or rarefaction wave connected with a stationary shock wave which satisfies (4) at $x = 0$. There are different solution concepts and admissibility criteria for solutions. Some of them are the “interface entropy condition” ([1]), the “crossing condition” ([4]) and the “existence of admissible discrete shock profiles” condition ([7]). Admissibility conditions for a general flux shapes are given in paper [3]. Let us note that in all

these cases the primary assumption is that the Rankine–Hugoniot condition is satisfied at the discontinuity point. In [9], the interface admissibility conditions are extended to so-called “convex-concave” fluxes when one of them, f_l or f_r is of convex type, and the other one is of concave type. The authors look at the case when f_l, f_r cross each other in some points X and Y , and take initial data from the interval $[X, Y]$. The existence of solutions consisting of a backward and a forward shock or rarefaction wave connected with a stationary shock at $x = 0$ is proved in this case.

In [2], equation (1) is considered in the context of certain flux geometries and sets of initial data for which the Rankine-Hugoniot condition at $x = 0$ cannot be satisfied, i.e. the above conditions are not met. For example, when f_l is of convex type and f_r of concave type and $f_l(u) > f_r(u)$ for all $u \in \Omega$, or when both fluxes are affine and $f_l' > 0 > f_r'$. The authors replace the Rankine-Hugoniot condition with a relaxed “generalized Rankine-Hugoniot condition” and accordingly define bounded “generalized entropy solutions” (GES) which can be obtained as limits of a modified Godunov type finite difference scheme. In the aforementioned cases, the generalized entropy condition reads as $f_l(u^-) \geq f_r(u^+)$ and GES just reflects the initial value discontinuity provided it satisfies the overcompressibility condition (6). Relaxed solutions obtained in such a way do not satisfy equation (1) in the distributional sense. These results are compared with the ones obtained by using the staggered mesh Godunov type scheme in [5]. They stated that in the observed cases this scheme gives a “big overshoot” at $x = 0$, but coincides with GES apart from the “overshoot”. We try to give another explanation of that phenomena. The Rankine–Hugoniot deficit (when the condition can not be satisfied) is connected with non–bounded generalized solutions containing the Dirac delta function (delta, singular shocks, etc.). We use shadow waves ([10]) in order to obtain a solution. The shadow wave solution concept relies on representing singular solutions by nets of piecewise constant functions. The basic idea in constructing stationary shadow waves at $x = 0$ is the perturbation of the speed $c = 0$ of a wave with the states u_0, u_1 from the left and right side of the wave by a small parameter ε . After the perturbation, the states u_0, u_1 of the original wave are connected by three shocks: The first one connects u_0 and $u_{0,\varepsilon}$, the second $u_{0,\varepsilon}$ with $u_{1,\varepsilon}$, while $u_{1,\varepsilon}$ and u_1 are connected by the third one. The middle wave has zero speed for $\varepsilon \ll 1$, whereas the others have a speed of order ε . The two intermediate states $u_{0,\varepsilon}$ and $u_{1,\varepsilon}$ tend to infinity when $\varepsilon \rightarrow 0$, and the solution tends to a singular shock wave or a delta shock wave (see Definition 1.3 below). All calculations are made in the sense of distributions by using Rankine-Hugoniot conditions, i.e. the equality is taken to be the equality of the distributional limit, (see Section 1.1). For comparison, one can see Fig. 2 as a representation of shadow waves and GES solutions obtained by numerical procedures. A precise definition of a shadow wave is given in Section 1.1. The Rankine-Hugoniot deficit in this case is

$$\kappa := f_l(u_0) - f_r(u_1), \tag{7}$$

and there is a solution in the form of a stationary shadow wave for nonzero Rankine-Hugoniot deficit at $x = 0$.

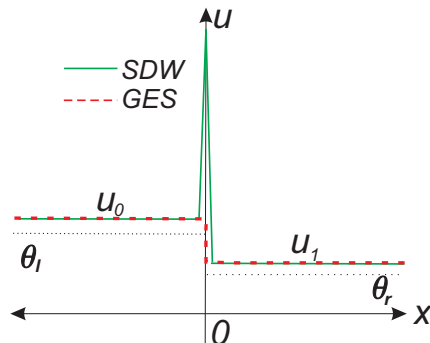


Figure 2: Shadow waves vs. GES

Relation (6) is taken to be the admissibility criterion which means that all the characteristics run into the shock wave from both sides. It is called the overcompressibility condition in the sequel. Later in the paper, we consider a more general set of initial data

$$u(x, 0) = \begin{cases} u_l, & x < 0 \\ u_r, & x > 0 \end{cases} \quad (8)$$

which may not satisfy condition (6). In this case, the states u_l and u_r have to be connected first by classical waves with some states u_0 and u_1 respectively, which satisfy condition (6). The speed of the wave connecting u_l and u_0 has to be non-positive, whereas the speed of the wave connecting u_1 and u_r has to be non-negative, of course. That condition provides a unique choice of the states u_0 and u_1 , as one will see in Section 2.2.

This paper is organized in the following way. Suppose that f_l is of convex type, f_r of concave type and $f_l(u) > f_r(u)$ for all u . After some introductory facts and giving assumptions on the flux geometry in Section 1.1, we prove the existence of shadow waves for (1), (3), (6) in the overcompressive case, in Section 2.1. In Section 2.2, the results are extended to the general Riemann problem. Then we consider our results to equation (1) in the case of linear fluxes in Section 2.3. Finally, in Section 2.4, Eq. (1) is rewritten in the form of a system of conservation laws and solved numerically using Godunov's scheme. It is an experimental verification that the obtained unbounded solution agrees with the theoretically expected shadow wave, obtained by using the numerical test from [6].

1.1 Preliminaries

Let us fix the notation and assumptions used in the paper. As already mentioned in the introduction, we are dealing with flux geometries for which the Rankine-Hugoniot condition cannot be satisfied. For simplicity, we will consider only the

case when $f_l(u) > f_r(u)$ and the fluxes are of convex or concave type. These two function types are described in the following definition.

Definition 1.1 *Let $f \in C^1(\Omega)$, $\Omega \subset \mathbb{R}$. Then f is said to be a convex type flux if it has one minimum and no maximum in Ω , a concave type flux if it has one maximum and no minimum in Ω .*

The following four cases are possible, as shown in Fig. 1:

- Case A: f_l is of convex type and f_r is of concave type,
- Case B: both f_l and f_r are of convex type,
- Case C: f_l is of concave type and f_r is of convex type,
- Case D: both f_l and f_r are of concave type.

Note that by Definition 1.1, convex (concave) type fluxes need not to be convex (concave) functions, see Fig. 1. The analysis of the solution of Eq. (1) is very similar in all the cases A-D, so we consider only the flux geometry in Case A:

Assumption 1: f_l is of convex type, f_r is of concave type and $f_l(u) > f_r(u)$ for all $u \in \Omega$.

Let us denote a unique minimum of f_l with θ_l and a maximum of f_r with θ_r , i.e. $f_l(\theta_l) = \min_{u \in \Omega} f_l(u)$ and $f_r(\theta_r) = \max_{u \in \Omega} f_r(u)$. We say that $f(u) \sim u^\nu$ if there exists a constant $c \in (0, +\infty)$ such that $\lim_{u \rightarrow \infty} \frac{f(u)}{u^\nu} = c$.

Let $f_{1,\varepsilon}, f_{2,\varepsilon}$ be nets of locally integrable functions over some domain $\omega \subset \mathbb{R} \times \mathbb{R}_+$, and $\mathcal{D}'(\omega)$ the space of distributions. The relation \approx is defined by $f_{1,\varepsilon} \approx f_1 \in \mathcal{D}'(\omega)$ if $\int_\omega f_{1,\varepsilon} \varphi \rightarrow \langle f_1 \delta, \varphi \rangle$ as $\varepsilon \rightarrow 0$ for every test function $\varphi \in C_0^\infty(\omega)$. Here $f_{1,\varepsilon} \approx f_{2,\varepsilon}$ means $f_{1,\varepsilon} - f_{2,\varepsilon} \approx 0$ and we say that $f_{1,\varepsilon}$ and $f_{2,\varepsilon}$ are distributionally equal (have the same distributional limit).

As noted in the introduction, a solution of Eq. (1) containing stationary singular wave which fits the Rankine-Hugoniot deficit at $x = 0$ is expected to appear. We will represent singular solutions with shadow waves, nets of piecewise constant functions defined as follows.

Definition 1.2 ([10]) *A shadow wave is a net of functions*

$$u_\varepsilon(x, t) = \begin{cases} u_0, & x < (c - \varepsilon)t \\ u_{0,\varepsilon}, & (c - \varepsilon)t < x < ct \\ u_{1,\varepsilon}, & ct < x < (c + \varepsilon)t \\ u_1, & x > (c + \varepsilon)t \end{cases}, \quad (9)$$

where

$$u_{0,\varepsilon} \sim \varepsilon^{-\alpha}, \quad u_{1,\varepsilon} \sim \varepsilon^{-\beta}, \quad (10)$$

and $\alpha, \beta \geq 0$. We call $u_{0,\varepsilon}$ and $u_{1,\varepsilon}$ intermediate states, and c presents the speed of the shadow wave.

A speed of a stationary shadow wave equals zero, i.e. $c = 0$ in (9). The value $k_\varepsilon(t) = \varepsilon u_{0,\varepsilon} t + \varepsilon u_{1,\varepsilon} t$ is called strength of the shadow wave. A shadow wave

is called weakly unique if all solutions have the same distributional limit. Here, uniqueness means that $\lim_{\varepsilon \rightarrow 0} k_\varepsilon(t) = k(t)$ is unique. A limit has the form

$$u(x, t) \approx \begin{cases} u_0, & x < 0 \\ u_1, & x > 0 \end{cases} + k(t)\delta(x),$$

where $\delta(x)$ is the Dirac delta function. The definition below defines when a singular solution obtained as a limit of a shadow wave as $\varepsilon \rightarrow 0$ is a delta shock or a singular shock wave.

Definition 1.3 ([10]) *If $\alpha = 1$ or $\beta = 1$ in (10), then $u_{0,\varepsilon}, u_{1,\varepsilon}$ are “major” or ε^{-1} components. Otherwise, if either $0 < \alpha < 1$ or $0 < \beta < 1$ then the corresponding component $u_{0,\varepsilon}$ or $u_{1,\varepsilon}$ is called a “minor component”.*

A delta shock wave is a shadow wave associated with a δ distribution with all minor components having finite limits as $\varepsilon \rightarrow 0$.

A singular shock wave has the feature that either $|u_{0,\varepsilon}| \rightarrow \infty$ and $\varepsilon |u_{0,\varepsilon}| \rightarrow 0$ or $|u_{1,\varepsilon}| \rightarrow \infty$ and $\varepsilon |u_{1,\varepsilon}| \rightarrow 0$ when $\varepsilon \rightarrow 0$.

2 Shadow Waves for the Two-Flux Equation

We start by considering the overcompressive case, i.e. when (6) is satisfied together with Assumption 1. Suppose that all assumptions from Section 1.1 are satisfied. For a solution, we look at the set of all elementary waves plus a shadow wave.

2.1 Existence of shadow waves in the overcompressive case

Let f from Eq. (1) with the initial data (3) satisfy condition (6). Then, there is a unique solution in the form of a stationary shadow wave.

Theorem 2.1 *Let*

$$f_l(u) \sim u^{\nu_1}, \quad f_r(u) \sim \chi u^{\nu_2}, \quad \text{as } u \rightarrow \infty, \quad (11)$$

where $\nu_1, \nu_2 \geq 0$, $\chi \in \{-1, 1\}$ and

$$\begin{aligned} \min(\nu_1, \nu_2) < 1 & \quad \text{if } \chi = 1, \\ \text{and } \nu_1 = \nu_2 \in [0, 2) & \quad \text{if } \chi = -1. \end{aligned} \quad (12)$$

Equation (1) together with the initial data of the form (3) satisfying (6) has a shadow wave as a solution which tends to a singular wave featuring the Dirac δ function

$$u(x, t) \approx \begin{cases} u_0, & x < 0 \\ u_1, & x > 0 \end{cases} + \kappa t \delta(x), \quad (13)$$

where κ is given by (7).

Proof: Substitute

$$u_\varepsilon(x, t) = \begin{cases} u_0, & x < -\varepsilon t \\ u_{0,\varepsilon}, & -\varepsilon t < x < 0 \\ u_{1,\varepsilon}, & 0 < x < \varepsilon t \\ u_1, & x > \varepsilon t \end{cases} \quad (14)$$

with

$$u_{0,\varepsilon} = u_0 + \xi_0 \varepsilon^{-\alpha} \text{ and } u_{1,\varepsilon} = u_1 + \xi_1 \varepsilon^{-\beta}$$

and $\alpha, \beta \geq 0, 0 \leq \xi_0, \xi_1 < \infty$ in (1).

From (14) and (2), using the standard Rankine-Hugoniot shock calculations we obtain

$$\langle \partial_t u_\varepsilon, \varphi(x, t) \rangle \approx \varepsilon \int_0^\infty (u_{0,\varepsilon} - u_0) \varphi(-\varepsilon t, t) dt - \varepsilon \int_0^\infty (u_1 - u_{1,\varepsilon}) \varphi(\varepsilon t, t) dt.$$

Using the Taylor expansion

$$\varphi(\pm \varepsilon t, t) = \varphi(0, t) + \sum_{j=1}^m \partial_x^j \varphi(0, t) \frac{(\pm \varepsilon t)^j}{j!} + \mathcal{O}(\varepsilon^{m+1}), \quad (15)$$

for $m = 1$, we obtain

$$\begin{aligned} \langle \partial_t u_\varepsilon, \varphi(x, t) \rangle &\approx \int_0^\infty (-\varepsilon(u_0 + u_1) + \varepsilon(u_{0,\varepsilon} + u_{1,\varepsilon})) \varphi(0, t) dx dt \\ &\quad + \int_0^\infty \varepsilon^2 (u_1 - u_0 + u_{0,\varepsilon} - u_{1,\varepsilon}) t \varphi_x(0, t) dx dt \\ &\approx \langle (-\varepsilon(u_0 + u_1) + \varepsilon(u_{0,\varepsilon} + u_{1,\varepsilon})) \delta(x), \varphi(x, t) \rangle \\ &\quad - \langle \varepsilon^2 (u_1 - u_0 + u_{0,\varepsilon} - u_{1,\varepsilon}) t \delta'(x), \varphi(x, t) \rangle. \end{aligned}$$

After neglecting all the terms tending to zero, we have

$$\begin{aligned} \langle \partial_t u_\varepsilon, \varphi(x, t) \rangle &\approx (\varepsilon^{1-\alpha} \xi_0 + \varepsilon^{1-\beta} \xi_1) \langle \delta(x), \varphi(x, t) \rangle \\ &\quad - (\varepsilon^{2-\alpha} \xi_0 - \varepsilon^{2-\beta} \xi_1) \langle t \delta'(x), \varphi(x, t) \rangle. \end{aligned} \quad (16)$$

Next,

$$\begin{aligned} \langle \partial_x f(u_\varepsilon), \varphi(x, t) \rangle &\approx \int_0^\infty (f_l(u_{0,\varepsilon}) - f_l(u_0)) \varphi(-\varepsilon t, t) dt \\ &\quad + \int_0^\infty (f_r(u_{1,\varepsilon}) - f_l(u_{0,\varepsilon})) \varphi(0, t) dt + \int_0^\infty (f_r(u_1) - f_r(u_{1,\varepsilon})) \varphi(\varepsilon t, t) dt. \end{aligned}$$

We have to use the Taylor expansion (15) for $m = 2$ now since there is a

term with ε^2 above. Using (7) we have

$$\begin{aligned}
\langle \partial_x f(u_\varepsilon), \varphi(x, t) \rangle &\approx - \int_0^\infty \kappa \varphi(0, t) dt - \varepsilon \int_0^\infty (f_l(u_{0,\varepsilon}) + f_r(u_{1,\varepsilon})) t \varphi_x(0, t) dt \\
&\quad + \frac{\varepsilon^2}{2} \int_0^\infty (f_l(u_{0,\varepsilon}) - f_r(u_{1,\varepsilon})) t^2 \varphi_{xx}(0, t) dt \\
&\approx \langle -\kappa \delta(x), \varphi(x, t) \rangle + \langle \varepsilon t (f_l(u_{0,\varepsilon}) + f_r(u_{1,\varepsilon})) \delta'(x), \varphi(x, t) \rangle \\
&\quad - \langle \frac{\varepsilon^2 t^2}{2} (f_l(u_{0,\varepsilon}) - f_r(u_{1,\varepsilon})) \delta''(x), \varphi(x, t) \rangle.
\end{aligned} \tag{17}$$

Note that $\kappa > 0$ due to Assumption 1. Thus, from (1), (16) and (17)

$$\begin{aligned}
\langle \partial_t u_\varepsilon + \partial_x f(u_\varepsilon), \varphi(x, t) \rangle &\approx \langle (-\kappa + (\xi_0 \varepsilon^{1-\alpha} + \xi_1 \varepsilon^{1-\beta})) \delta(x), \varphi(x, t) \rangle \\
&\quad + \langle (\varepsilon (f_l(u_{0,\varepsilon}) + f_r(u_{1,\varepsilon})) - (\xi_0 \varepsilon^{2-\alpha} - \xi_1 \varepsilon^{2-\beta})) t \delta'(x), \varphi(x, t) \rangle \\
&\quad - \langle \frac{\varepsilon^2 t^2}{2} (f_l(u_{0,\varepsilon}) - f_r(u_{1,\varepsilon})) \delta''(x), \varphi(x, t) \rangle \approx 0.
\end{aligned}$$

These relations are satisfied if the following holds

$$\lim_{\varepsilon \rightarrow 0} ((\xi_0 \varepsilon^{1-\alpha} + \xi_1 \varepsilon^{1-\beta})) = \kappa \tag{18}$$

$$\lim_{\varepsilon \rightarrow 0} (\varepsilon (f_l(u_{0,\varepsilon}) + f_r(u_{1,\varepsilon})) - (\xi_0 \varepsilon^{2-\alpha} - \xi_1 \varepsilon^{2-\beta})) = 0 \tag{19}$$

$$\lim_{\varepsilon \rightarrow 0} \varepsilon^2 (f_l(u_{0,\varepsilon}) - f_r(u_{1,\varepsilon})) = 0. \tag{20}$$

Let us consider relation (18) first. It is clear that $\alpha, \beta \leq 1$ since the left-hand side would be infinite otherwise (note that $\xi_0, \xi_1 \geq 0$). This implies that the second term on the left-hand side of relation (19) vanishes, i.e. relation (19) becomes

$$\lim_{\varepsilon \rightarrow 0} \varepsilon (f_l(u_{0,\varepsilon}) + f_r(u_{1,\varepsilon})) = 0$$

and system (18)-(20) becomes

$$\begin{aligned}
\lim_{\varepsilon \rightarrow 0} ((\xi_0 \varepsilon^{1-\alpha} + \xi_1 \varepsilon^{1-\beta})) &= \kappa \\
\lim_{\varepsilon \rightarrow 0} \varepsilon (f_l(u_{0,\varepsilon}) + f_r(u_{1,\varepsilon})) &= 0 \\
\lim_{\varepsilon \rightarrow 0} \varepsilon^2 (f_l(u_{0,\varepsilon}) - f_r(u_{1,\varepsilon})) &= 0.
\end{aligned}$$

It is clear that at least one of the parameters α or β should be 1 since $\kappa > 0$. Taking into account (11), the above system becomes

$$\xi_0 \varepsilon^{1-\alpha} + \xi_1 \varepsilon^{1-\beta} \approx \kappa \tag{21}$$

$$c_1 \xi_0^{\nu_1} \varepsilon^{1-\nu_1 \alpha} + \chi c_2 \xi_1^{\nu_2} \varepsilon^{1-\nu_2 \beta} \approx 0 \tag{22}$$

$$c_1 \xi_0^{\nu_1} \varepsilon^{2-\nu_1 \alpha} - \chi c_2 \xi_1^{\nu_2} \varepsilon^{2-\nu_2 \beta} \approx 0, \tag{23}$$

where $c_1, c_2 > 0$ are constants depending on the behavior of f_l at infinity. The fluxes f_l and f_r satisfy (12) and $\alpha = 1$ or $\beta = 1$, so one can easily check that the system (21–23) is consistent.

Case 1. Let us first consider the case $\chi = 1$. System (21–23) is then

$$\begin{aligned}\xi_0 \varepsilon^{1-\alpha} + \xi_1 \varepsilon^{1-\beta} &\approx \kappa \\ c_1 \xi_0^{\nu_1} \varepsilon^{1-\nu_1 \alpha} + c_2 \xi_1^{\nu_2} \varepsilon^{1-\nu_2 \beta} &\approx 0 \\ c_1 \xi_0^{\nu_1} \varepsilon^{2-\nu_1 \alpha} - c_2 \xi_1^{\nu_2} \varepsilon^{2-\nu_2 \beta} &\approx 0.\end{aligned}$$

If both $\nu_1 < 1$ and $\nu_2 < 1$, then the above conditions are satisfied for $\alpha = \beta = 1$ and $\xi_0 + \xi_1 = \kappa$. On the other hand, if $\nu_1 < 1$ and $\nu_2 \geq 1$, then the conditions are satisfied for $\alpha = 1$, $\beta = 0$, $\xi_0 = \kappa$ and $\xi_1 = 0$. Similarly, if $\nu_1 \geq 1$ and $\nu_2 < 1$, then (21–23) holds for $\alpha = 0$, $\beta = 1$, $\xi_0 = 0$ and $\xi_1 = \kappa$.

Case 2. Let us now suppose that $\chi = -1$. System (21–23) then becomes

$$\begin{aligned}\xi_0 \varepsilon^{1-\alpha} + \xi_1 \varepsilon^{1-\beta} &\approx \kappa \\ c_1 \xi_0^{\nu_1} \varepsilon^{1-\nu_1 \alpha} - c_2 \xi_1^{\nu_2} \varepsilon^{1-\nu_2 \beta} &\approx 0 \\ c_1 \xi_0^{\nu_1} \varepsilon^{2-\nu_1 \alpha} + c_2 \xi_1^{\nu_2} \varepsilon^{2-\nu_2 \beta} &\approx 0.\end{aligned}$$

If $\nu_1 < 1$ and $\nu_2 < 1$, $\nu_1 < 1$ and $\nu_2 \geq 1$ or $\nu_1 \geq 1$ and $\nu_2 < 1$ we have the same results under the same conditions in as in Case 1.

If $\nu_1 = 1$ and $\nu_2 \geq 1$, one can easily see that system (21–23) is satisfied provided

$$\alpha = 1, \beta = \frac{1}{\nu_2}, \xi_0 = \kappa \text{ and } \xi_1 = \left(\frac{c_1}{c_2} \kappa \right)^{\frac{1}{\nu_2}},$$

whereas for $\nu_1 \geq 1$ and $\nu_2 = 1$ we obtain $\alpha = \frac{1}{\nu_1}$, $\beta = 1$, $\xi_0 = \left(\frac{c_2}{c_1} \kappa \right)^{\frac{1}{\nu_1}}$ and $\xi_1 = \kappa$.

If $\nu_1 = \nu_2 \in [1, 2)$, for $\alpha = \beta = 1$, one gets ξ_0, ξ_1 from the system

$$\begin{aligned}\xi_0 + \xi_1 &= \kappa \\ c_1 \xi_0^{\nu_1} - c_2 \xi_1^{\nu_1} &= 0,\end{aligned}$$

i.e.,

$$\xi_0 = \frac{\kappa \left(\frac{c_2}{c_1} \right)^{\frac{1}{\nu_1}}}{1 + \left(\frac{c_2}{c_1} \right)^{\frac{1}{\nu_1}}}, \quad \xi_1 = \frac{\kappa}{1 + \left(\frac{c_2}{c_1} \right)^{\frac{1}{\nu_1}}}.$$

On the other hand, if $\nu_1 \neq \nu_2 \in [1, 2)$, we have two cases to consider: $\nu_1 < \nu_2$ and $\nu_1 > \nu_2$. Let $\nu_1 < \nu_2$. Then system (21–23) is satisfied for $\alpha = 1$, $\beta = \frac{\nu_1}{\nu_2}$,

$\xi_0 = \kappa$ and $\xi_1 = \left(\frac{c_1}{c_2} \kappa^{\nu_1} \right)^{\frac{1}{\nu_2}}$. Similarly, if $\nu_1 > \nu_2$ one gets that the conditions

are satisfied for $\alpha = \frac{\nu_2}{\nu_1}$, $\beta = 1$, $\xi_0 = \left(\frac{c_2}{c_1} \kappa^{\nu_2} \right)^{\frac{1}{\nu_1}}$ and $\xi_1 = \kappa$. \square

ν_1, ν_2	Solution of system (21–23)	Shadow wave when $\varepsilon \rightarrow 0$
Case 1: $\chi = 1$		
$\nu_1 < 1, \nu_2 < 1$	$\alpha = \beta = 1, \xi_1 + \xi_2 = \kappa$	delta shock wave
$\nu_1 < 1, \nu_2 \geq 1$	$\alpha = 1, \beta = 0, \xi_0 = \kappa, \xi_1 = 0$	delta shock wave
$\nu_1 \geq 1, \nu_2 < 1$	$\alpha = 0, \beta = 1, \xi_0 = 0, \xi_1 = \kappa$	delta shock wave
Case 2: $\chi = -1$		
$\nu_1 < 1, \nu_2 < 1$	$\alpha = \beta = 1, \xi_1 + \xi_2 = \kappa$	delta shock wave
$\nu_1 < 1, \nu_2 \geq 1$	$\alpha = 1, \beta = 0, \xi_0 = \kappa, \xi_1 = 0$	delta shock wave
$\nu_1 \geq 1, \nu_2 < 1$	$\alpha = 0, \beta = 1, \xi_0 = 0, \xi_1 = \kappa$	delta shock wave
$\nu_1 = 1, \nu_2 \geq 1$	$\alpha = 1, \beta = \frac{1}{\nu_2}, \xi_0 = \kappa, \xi_1 = \left(\frac{c_1}{c_2}\kappa\right)^{\frac{1}{\nu_2}}$	singular shock wave
$\nu_1 \geq 1, \nu_2 = 1$	$\alpha = \frac{1}{\nu_1}, \beta = 1, \xi_0 = \left(\frac{c_2}{c_1}\kappa\right)^{\frac{1}{\nu_1}}, \xi_1 = \kappa$	singular shock wave
$\nu_1 = \nu_2 \in [1, 2)$	$\alpha = \beta = 1,$ $\xi_0 = \frac{\kappa \left(\frac{c_2}{c_1}\right)^{\frac{1}{\nu_1}}}{\left(1 + \frac{c_2}{c_1}\right)^{\frac{1}{\nu_1}}}, \xi_1 = \frac{\kappa}{\left(1 + \frac{c_2}{c_1}\right)^{\frac{1}{\nu_1}}}$	delta shock wave
$\nu_1, \nu_2 \in [1, 2),$ $\nu_1 < \nu_2$	$\alpha = 1, \beta = \frac{\nu_1}{\nu_2},$ $\xi_0 = \kappa, \xi_1 = \left(\frac{c_1}{c_2}\kappa^{\nu_1}\right)^{\frac{1}{\nu_2}}$	singular shock wave
$\nu_1, \nu_2 \in [1, 2),$ $\nu_1 > \nu_2$	$\alpha = \frac{\nu_2}{\nu_1}, \beta = 1,$ $\xi_0 = \left(\frac{c_2}{c_1}\kappa^{\nu_2}\right)^{\frac{1}{\nu_1}}, \xi_1 = \kappa$	singular shock wave

Table 1: The limits of the shadow wave solution in various cases when $\varepsilon \rightarrow 0$

The limits of obtained shadow waves as $\varepsilon \rightarrow 0$ are given in Table 1 according to Definition 1.3.

Example 2.1 *Let*

$$f_l(u) = \frac{1 + 2u^2}{1 + u^2}, \quad f_r(u) = -\frac{1 + 2u^2}{1 + u^2}, \quad (24)$$

and $u_0(x) = 1$.

One can easily check that $f_l'(1) > 0 > f_r'(1)$, i.e. that the overcompressibility condition is satisfied. Using that $\kappa = f_l(1) - f_r(1) = 3$, $\chi = -1$, $\nu_1 < 1$ and $\nu_2 < 1$ and Theorem 2.1, we obtain a solution in the form of a stationary shadow

wave (i.e. delta shock wave, see Table 1) with the strength equal to $k_\varepsilon(t) = 3t$,

$$u(x, t) \approx 1 + 3t\delta(x).$$

Example 2.2 Let

$$f_l(u) = \sqrt{u^2 + 1} + 1, \quad f_r(u) = \frac{1}{\sqrt{u^2 + 1}},$$

and $u_0(x) = 1$.

In this case we have $\nu_1 \geq 1, \nu_2 < 1$ and $\chi = 1$. Thus we obtain a delta shock wave of the form

$$u(x, t) \approx 1 + \frac{2 + \sqrt{2}}{2}t\delta(x).$$

2.2 Solutions to Riemann problem

Let us now consider problem (1) with a general Riemann initial data

$$u(x, 0) = \begin{cases} u_l, & x < 0 \\ u_r, & x > 0 \end{cases}.$$

There are the four possible positions of the initial data states u_l, u_r with respect to θ_l, θ_r :

- i) $u_l \geq \theta_l, u_r \geq \theta_r$
- ii) $u_l \geq \theta_l, u_r < \theta_r$
- iii) $u_l < \theta_l, u_r \geq \theta_r$
- iv) $u_l < \theta_l, u_r < \theta_r$

due to Assumption 1. One can see the illustration at Fig. 3.

In case i), the overcompressibility condition (6) is satisfied and there exists a stationary shadow wave at $x = 0$ with the states u_l, u_r . We will denote it by $SDW^0(u_l, u_r)$. Note that in this case the shadow wave is uniquely determined. Namely, if there would exist a state $\hat{u}_r > \theta_r$ and $\hat{u}_r \neq u_r$ that determines a stationary shadow wave at $x = 0$, i.e. $SDW^0(u_l, \hat{u}_r)$, then the pair (\hat{u}_r, u_r) would determine a wave of the right-hand side of $x = 0$ propagating to left since $f'_r(\hat{u}), f'_r(\hat{u}_r) \leq 0$, but that is impossible.

In case ii), we have $f'_l(u_l) > 0, f'_r(u_r) > 0$, i.e. the overcompressibility condition is violated. Thus, a state u_r has to be connected with a state u_1 , such that $f'_r(u_1) \leq 0$, i.e. $u_1 \geq \theta_r$. Then the pair u_l, u_1 satisfies the overcompressibility condition and Theorem 2.1 implies the existence of a $SDW^0(u_l, u_1)$. The states u_l and u_1 are then connected with a forward wave that is in fact a rarefaction wave since $u_1 > u_r$ and f_r is of concave type. The unique choice of the state u_1 is $u_1 = \theta_r$ since for any $u_1 > \theta_r$ we would have $f'_r(u_r) > 0, f'_r(u_1) < 0$, but that is not allowed, too. Thus, a unique solution is of the form $SDW^0(u_l, \theta_r) + \vec{R}(\theta_r, u_r)$ in this case. Here $\vec{R}(u_1, u_r)$ denotes the forward rarefaction wave and “+” means “followed by”.

Similarly, the only proper choice is $u_0 = \theta_l$ in case iii). It is connected to u_l in such a way that the pair (u_l, u_0) satisfies the overcompressibility condition.

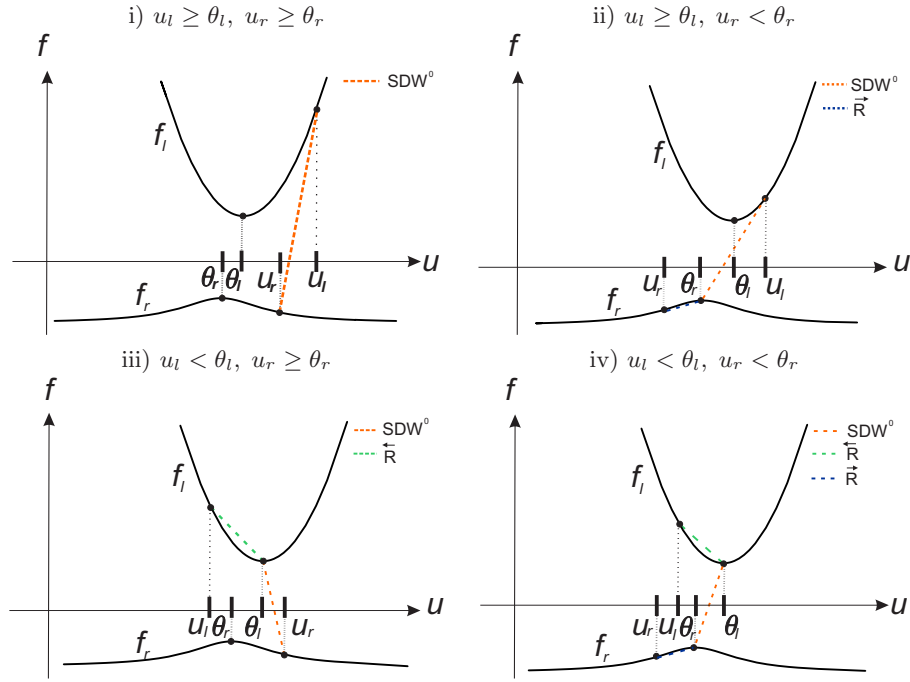


Figure 3: Various positions of initial data states u_l, u_r with respect to θ_l, θ_r

Also, there is no interaction of the backward rarefaction wave $\overleftarrow{R}(u_l, u_0)$ with the $SDW^0(u_0, u_r)$.

Case iv) is a combination of the previous cases. A unique solution is a wave combination $\overleftarrow{R}(u_l, \theta_l) + SDW^0(\theta_l, \theta_r) + \vec{R}(\theta_r, u_r)$.

Table 2 shows solutions of the Riemann problem for (1), (8) in cases i)-iv).

Subcase	Position of u_l, u_r	Solution
i)	$u_l \geq \theta_l$ and $u_r \geq \theta_r$	$SDW^0(u_l, u_r)$
ii)	$u_l \geq \theta_l$ and $u_r < \theta_r$	$SDW^0(u_l, \theta_r) + \vec{R}(\theta_r, u_r)$
iii)	$u_l < \theta_l$ and $u_r \geq \theta_r$	$\overleftarrow{R}(u_l, \theta_l) + SDW^0(\theta_l, u_r)$
iv)	$u_l < \theta_l$ and $u_r < \theta_r$	$\overleftarrow{R}(u_l, \theta_l) + SDW^0(\theta_l, \theta_r) + \vec{R}(\theta_r, u_r)$

Table 2: Solutions of problem (1), (8)

2.3 Remark on the linear case

Suppose that both fluxes are affine. The above method with a centered shadow wave can also be applied. As we mentioned in the introduction, when both fluxes are linear and $f'_l > 0 > f'_r$, there exists no classical solution for arbitrary initial values u_l, u_r since any pair (u^-, u^+) (u^- and u^+ are given by (5)) which satisfies the Rankine-Hugoniot jump condition at $x = 0$ determines a wave connecting u_l and u^- at the left-hand side of the origin traveling to right, and a right-hand side wave connecting u_r and u^+ traveling to left that are not allowed (see illustration in Fig. 4).

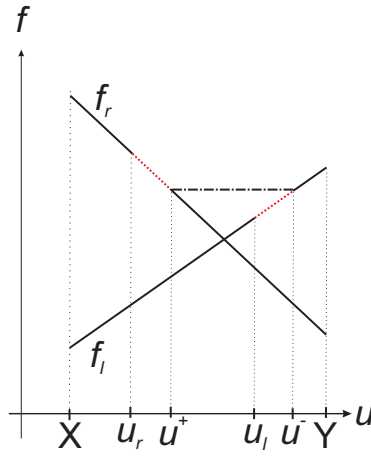


Figure 4: The overcompressive linear flux case

Put $f_l(u) = p_l u + q_l$, $f_r(u) = p_r u + q_r$ in Eq. (1) where $p_l \geq 0$, $p_r \leq 0$ and use the initial data (3). It is clear that

$$f'_l(u_0) > 0 > f'_r(u_1)$$

for every choice of the states u_0, u_1 . That fits the case $\chi = 1$, $\nu_1 = \nu_2 \in [1, 2)$ (see Table 1), i.e. $\alpha = 1$, $\beta = 1$, $\xi_0 = \frac{\kappa \left(\frac{c_2^2}{c_1}\right)}{1 + \frac{c_2^2}{c_1}}$ and $\xi_1 = \frac{\kappa}{1 + \left(\frac{c_2^2}{c_1}\right)}$.

On the other hand, the Rankine-Hugoniot deficit equals

$$\kappa = f_l(u_0) - f_r(u_1) = p_l u_0 + q_l - p_r u_1 - q_r.$$

According to Theorem 2.1, the problem has a solution in the form of a $SDW^0(u_0, u_1)$ tending to a delta shock wave as $\varepsilon \rightarrow 0$, i.e.

$$u(x, t) \approx U + (p_l u_0 - p_r u_1 + q_l - q_r) t \delta(x), \quad (25)$$

where we denoted (3) with $U(x)$, i.e.

$$U(x) = \begin{cases} u_0, & x < 0 \\ u_1, & x > 0 \end{cases}.$$

Example 2.3 Let us consider Eq. (1) where the fluxes are given by

$$f_l = u \quad \text{and} \quad f_r = -u \quad (26)$$

together with the constant initial data $u(x, 0) = 1$.

According to (25), problem (1), (26) has a solution in the form $SDW^0(1, 1)$ with the strength $\kappa t = (f_l(1) - f_r(1))t = 2t$. As we can see from Table 1, the obtained shadow wave is a delta shock wave.

The case with linear fluxes is convenient for using the delta split solution concept [11, 12], so one could derive a delta shock wave solution on an alternative way and compare it with the solution obtained using shadow waves.

2.4 A numerical example

We will use the well known Godunov method for the numerical example bellow. Take

$$v_t + F(v)_x = 0, \quad (27)$$

with $v = (v^1, v^2)$ being a two component vector with components $v^i : \mathbb{R} \times \mathbb{R}_+ \rightarrow \mathbb{R}$, $i = 1, 2$ and $F : \mathbb{R}^2 \rightarrow \mathbb{R}^2$, be a nonlinear system of conservation laws together with the initial data

$$v(x, 0) = \begin{cases} v_l, & x < 0 \\ v_r, & x > 0 \end{cases},$$

where $v_l = (v_l^1, v_l^2)$ and $v_r = (v_r^1, v_r^2)$. Solving system (27) numerically starts by discretizing the $x - t$ plane using a uniform grid $\Delta x \mathbb{Z} \times \Delta t \mathbb{N}$, $\Delta x > 0$, $\Delta t > 0$ with grid points labeled $(x_j, t_n) := (j\Delta x, n\Delta t)$, the discrete unknowns $u_j^n = u(x_j, t_n)$, and using a suitable numerical scheme subsequently. Herein, we use Godunov's method coupled with Roe's linearization (see [8]). The basic principle of the method can be described as follows. First, system (27) is linearized by approximating system (27) locally at each cell interface

$$v_t + \widehat{A}_{j-1/2} v_x = 0, \quad (28)$$

where $\widehat{A}_{j-1/2}$ is a 2×2 matrix that approximate $F'(v)$ in the neighborhood of v_{j-1} and v_j having the following properties:

$$\widehat{A}_{j-1/2}(v_{j-1}, v_j)(v_j - v_{j-1}) = F(v_j) - F(v_{j-1}) \quad (29)$$

$$\widehat{A}_{j-1/2}(v_{j-1}, v_j) \quad \text{has real distinct eigenvalues} \quad (30)$$

$$\widehat{A}_{j-1/2}(v_{j-1}, v_j) \rightarrow F'(\bar{v}) \quad \text{when} \quad v_{j-1}, v_j \rightarrow \bar{v}. \quad (31)$$

Note that condition (30) implies that $\widehat{A}_{j-1/2}$ is diagonalizable, and it can be decomposed

$$\widehat{A}_{j-1/2} = R_{j-1/2} \Lambda_{j-1/2} R_{j-1/2}^{-1},$$

with $\Lambda_{j-1/2} = \text{diag}(\lambda_{j-1/2}^1, \lambda_{j-1/2}^2)$ being a diagonal matrix of eigenvalues and $R_{j-1/2} = [r_{j-1/2}^1 \mid r_{j-1/2}^2]$ being the matrix of appropriate eigenvectors. Let us introduce the following notation

$$\begin{aligned}\lambda_{j-1/2,i}^+ &= \max(\lambda_{j-1/2,i}, 0), \quad \Lambda_{j-1/2}^+ = \text{diag}(\lambda_{j-1/2,1}^+, \lambda_{j-1/2,2}^+), \\ \lambda_{j-1/2,i}^- &= \min(\lambda_{j-1/2,i}, 0), \quad \Lambda_{j-1/2}^- = \text{diag}(\lambda_{j-1/2,1}^-, \lambda_{j-1/2,2}^-), \\ \widehat{A}_{j-1/2}^+ &= R_{j-1/2} \Lambda_{j-1/2}^+ R_{j-1/2}^{-1}, \quad \widehat{A}_{j-1/2}^- = R_{j-1/2} \Lambda_{j-1/2}^- R_{j-1/2}^{-1}, \quad i = 1, 2.\end{aligned}$$

Now, for the linearized system (28) Godunov method takes the form

$$v_j^{n+1} = v_j^n - \frac{\Delta t_n}{\Delta x_j} \left[\widehat{A}_{j+1/2}^-(v_{j+1}^n - v_j^n) + \widehat{A}_{j-1/2}^+(v_j^n - v_{j-1}^n) \right]. \quad (32)$$

Let us verify the results obtained in Example 2.1 numerically. Suppose that (1) is the nonlinear system of conservation laws

$$\begin{aligned}u_t + (hf_r(u) + (1-h)f_l(u))_x &= 0 \\ h_t &= 0,\end{aligned} \quad (33)$$

with the initial data

$$u(x, 0) = 1, \quad h(x, 0) = \begin{cases} 0, & x < 0 \\ 1, & x > 0 \end{cases}.$$

The functions f_l, f_r are given by (24). Using the Roe linearization, system (33) is approximated by the linear system (28) at every cell interface where

$$\widehat{A}_{j-1/2} = \begin{bmatrix} \gamma_{j-1/2} & \rho_{j-1/2} \\ 0 & 0 \end{bmatrix},$$

and

$$\gamma_{j-1/2} = \frac{(1 - 2h_{j-1})(u_{j-1} + u_j)}{(1 + u_{j-1}^2)(1 + u_j^2)} \quad \text{and} \quad \rho_{j-1/2} = \frac{-2(1 + 2u_j^2)}{(1 + u_j^2)}.$$

The eigenvalues of $\widehat{A}_{j-1/2}$ are $\lambda_{j-1/2,1} = \gamma_{j-1/2}$ and $\lambda_{j-1/2,2} = 0$. One can easily check that conditions (29) and (31) are satisfied. Condition (30) also holds as $\gamma_{j-1/2} \neq 0$ for all j since $u_l + u_r = 2 > 0$ and the expected solution is a shadow wave above the line $u = 1$. This implies $u_{j-1} + u_j \neq 0$ for all j .

Now, we use Godunov's wave propagation method for linear systems of hyperbolic conservation laws (32) with a mesh size $\Delta x = 0.01$ and obtain results shown in Fig.5.

Note that the unknown h in system (33) is just an auxiliary variable, presenting in fact the discrete Heaviside function. As expected, h does not change during time. On the other hand, the numerical approximation of u is unbounded.

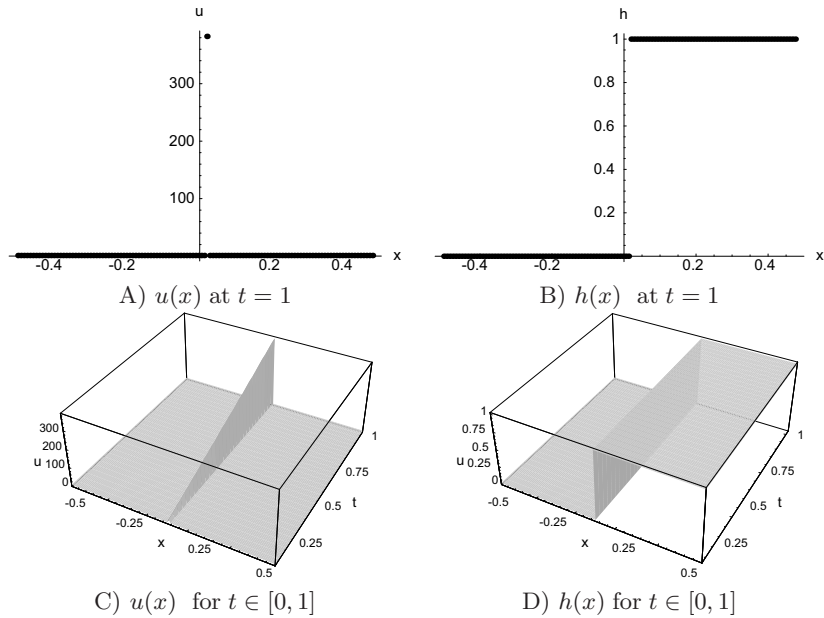


Figure 5: Numerical results for the problem in Ex. 2.1

In order to verify if it really presents a delta shock wave, we perform a test we first introduced in [6]. Denote the singular part of the expected delta shock wave (13) with u_s , i.e. $u_s = \kappa t$, where κ is given by (7). Next, denote the surface under a singular part of the solution with

$$P(t) = \int u_s dx = \kappa t \int \delta(x) dx \approx \kappa t = 3t,$$

since it is well known that $\int \delta(x) dx \approx 1$, and as seen in Example 2.1, in our case $\kappa = 3$. In our numerical test, we approximate $P(t)$ using the left Riemann sum, denoted with $P_l(t)$. As one can see in Fig. 6, the true (dashed line) and calculated (full line) surface under the singular part of the delta shock wave are very close over the interval $[0, 1]$, so we conclude that the obtained unbounded numerical result is actually the expected $SDW^0(1, 1)$.

References

- [1] A. Adimurthi, S. Mishra, G. D. V. Gowda, Optimal entropy solutions for conservation laws with discontinuous flux-functions, *J. Hyperbolic Differ. Equ.* **2** (2005) no.4 783–837.
- [2] Adimurthi, S. Mishra, G.D. Veerappa Gowda, Conservation law with the flux function discontinuous in the space variable – II, Convex-concave type

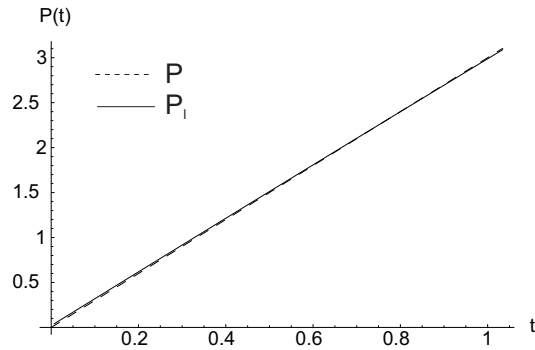


Figure 6: Delta shock wave verification test for the solution in Ex. 2.1

fluxes and generalized entropy solutions, *J. Comput. Appl. Math.* **203** (2007) 310–344.

- [3] B. Andreianov, C. Cancès, C. On interface transmission conditions for conservation laws with discontinuous flux of general shape, *Journal of hyperbolic differential equations* 12 (2015), 343–384.
- [4] R. Bürger, K. H. Karlsen, N. H. Risebro, J. D. Towers, Well-posedness in BV_t and convergence of a difference scheme for continuous sedimentation in ideal clarifier-thickener units, *Numer. Math.* (2004) 97: 25–65.
- [5] K. H. Karlsen, N. H. Risebro, J. D., Upwind difference approximations for degenerate parabolic convection-diffusion equations with a discontinuous coefficient, *IMA J. Numer. Anal.*, **22** (2002), no.4, 623–664.
- [6] Krejic N., Krunic T., Nedeljkov M., *Numerical verification of delta shock waves for pressureless gas dynamics*, Journal of Mathematical Analysis and Applications, vol 345, no 1, 243–257, (2008)
- [7] Krunic T., Nedeljkov M., *Discrete shock profiles for scalar conservation laws with discontinuous fluxes*, Journal of Mathematical Analysis and Applications, vol 435, Issue 1, 986–1010, (2016)
- [8] R. J. LeVeque, *Finite volume methods for hyperbolic problems*, Cambridge Texts in Applied Mathematics, Cambridge, United Kingdom, (2004) 317–323.
- [9] S. Mishra, *Convergence of upwind finite difference schemes for a scalar conservation law with indefinite discontinuities in the flux function*, *SIAM J. Numer. Anal.*, **vol 43** (2005), no.2, 559–577.
- [10] M. Nedeljkov, *Shadow waves: Entropies and interactions for delta and singular shocks*, *Arch. Rational Mech. Anal.*, **197** (2010), 489–537.

- [11] M. Nedeljkov, Unbounded solutions to some systems of conservation laws - split delta shock waves, *Mat. Ves.*, **54** (2002) 145–149.
- [12] M. Nedeljkov, M. Oberguggenberger, Interactions of delta shock waves in a strictly hyperbolic system of conservation laws, *J. Math. Anal. Appl.*, **344** (2008), no.2, 1143–1157.

Tanja Krunić
The Higher Education Technical School of Professional Studies Novi Sad, Serbia
email: krunic@vtsns.edu.rs

Marko Nedeljkov
Department of Mathematics and Informatics, Faculty of Sciences, University of Novi Sad, Serbia
email: marko@dmi.uns.ac.rs